Environmental Pollution 263 (2020) 114468

Contents lists available at ScienceDirect

Environmental Pollution

journal homepage: www.elsevier.com/locate/envpol

Differential histological, cellular and organism-wide response of earthworms exposed to multi-layer graphenes with different morphologies and hydrophobicity☆

Haiyun Zhang [a, b], Julia Vidonish [c], Weiguang Lv [a], Xilong Wang [b, *], Pedro Alvarez [d, **]

[a] Shanghai Academy of Agricultural Sciences, Shanghai, 201403, China
[b] College of Urban and Environmental Sciences, Peking University, Beijing, 100871, China
[c] Arcadis, 1100 Olive Way, Suite 800, Seattle, WA, 98101, United States
[d] Rice University, Houston, TX, 77005, United States

ARTICLE INFO

Article history:
Received 7 November 2019
Received in revised form
24 March 2020
Accepted 25 March 2020
Available online 1 April 2020

Keywords:
Multi-layer graphene
Morphology
Hydrophobicity
Earthworm response

ABSTRACT

The growing use of graphene-based nanomaterials (GBNs) for various applications increases the probability of their environmental releases and calls for a systematic assessment of their potential impacts on soil invertebrates that serve as an important link along terrestrial food chains. Here, we investigated the response of earthworms (*Eisenia fetida*) to three types of multi-layer graphenes (MLGs) (G1, G2 and G3 with 12–15 layers) with variable morphology (lateral sizes: 7.4 ± 0.3, 6.4 ± 0.1 and 2.8 ± 0.1 μm; thicknesses: 5.0 ± 0.1, 4.2 ± 0.1 and 4.0 ± 0.2 nm, respectively) and hydrophobicity ((O + N)/C ratios: 0.029, 0.044 and 0.075; contact angles: 122.8, 118.8 and 115.1°, respectively). Exposure to these materials was conducted for 28 days (except for 48-h avoidance test) separately in potting or farm soil at 0.2% and 1% by weight. Earthworms avoided both soils when amended with 1% of the smaller and more hydrophilic MLGs (G2 and G3), leading to a decreased trend in worm cocoon formation. The smallest and most hydrophilic MLG (G3), which was easier to assimilate, also significantly inhibited the viability (20.2–56.0%) and mitochondrial membrane potential (32.0–48.5%) of worm coelomocytes in both soils. In contrast, oxidative damage (indicated by lipid peroxides) was more pronounced upon exposure to more hydrophobic and larger graphenic materials (G1 and G2), which were attributed to facilitated adhesion to and disruption of worm membranes. These findings highlight the importance of MLG morphology and hydrophobicity in their potential toxicity and mode of action, as well as ecological risks associated with incidental and accidental releases.

1. Introduction

Graphene and graphene-based nanomaterials (GBNs) have received increasing attention due to their unique physicochemical properties, such as a large surface area, strong electrical and thermal conductivity, and high mechanical strength. Numerous applications have been developed in electronics, optoelectronics, energy conversion and storage, antimicrobial coatings, soil/wastewater remediation, and agricultural practices (Al-Hartomy et al., 2018; Gomes et al., 2018; Huang et al., 2019; Zhu et al., 2019). Many more graphene-enabled products are still under investigation, and the market value of such products is expected to reach $2.1 USD billion by 2025 (Katsumiti et al., 2017). With the growing commercial interest in GBN-enabled products, an increasing amount of these materials may inevitably be released to the environment, which underscores the need for a systematic risk assessment.

Most existing GBN ecotoxicity literature focuses on mammalian cells, aquatic organisms and plants in hydroponic systems (Akhavan et al., 2012; Lu et al., 2017; Malina et al., 2019; Peruzynska et al., 2017). These studies reveal the importance of hydrophobicity- and dimension-dependent effects on GBN toxicity to biota. However, such property-dependent effects have not been investigated for earthworm species, which represent 80% of the total biomass of soil fauna and are critical to soil and ecological health (Yang et al., 2018). Related earthworm nanotoxicity studies have mainly

☆ This paper has been recommended for acceptance by Bernd Nowack.
* Corresponding author.
** Corresponding author.
E-mail addresses: xilong@pku.edu.cn (X. Wang), alvarez@rice.edu (P. Alvarez).

https://doi.org/10.1016/j.envpol.2020.114468
0269-7491/

focused on concentration-dependent effects and bio-uptake, with most studies investigating carbonaceous nanomaterials such as C_{60} and carbon nanotubes. For instance, Li et al. (2010) observed a lower bioaccumulation factor in earthworms for C_{60} at higher doses of 60, 100 and 300 mg/kg (vs. a lower dose of 0.25 mg/kg), although significant avoidance or growth/cocoon inhibition was not observed at C_{60} dose of up to 10,000 mg/kg (Li and Alvarez, 2011). Pakarinen et al. (2011) similarly found little effect of 10 and 50 mg/kg C_{60} on worm survival or reproductive activities. Double-walled carbon nanotubes appear to be more toxic, and were reported to exert reproductive toxicity to *Eisenia veneta* via administration in the food at 37 mg/kg (Scott-Fordsmand et al., 2008). Calisi et al. (2016) observed high sensitivity of cellular and biochemical responses in *Eisenia fetida* to multi-walled carbon nanotubes at 30 and 300 mg/kg. In addition, Mao et al. (2016) demonstrated that protein coating decreased the size of few-layer graphenes, thereby effectively increasing graphene uptake by *Eisenia fetida*. This study highlighted the importance of surface coating on graphene in its uptake by earthworms, and pointed out that the specific hydrophobicity- and dimension-dependent effect remains largely unknown with these species.

In this work, earthworms (*Eisenia fetida*) were exposed to MLGs of dissimilar lateral size, thickness and hydrophobicity to discern the importance of these properties in their mode of action. Potting and farm soils were selected to represent two common habitats for earthworms and to enable a better understanding how soil properties may influence the effects of MLG exposure. Various biochemical parameters including histological (oxidative stress and peroxides), cellular/subcellular (coelomocyte viability and mitochondrial membrane potential), and organism-wide responses (avoidance and reproductive efficacy) were investigated as a function of exposure to advance understanding of the ecological risks of MLGs to soil biota and the potential links between various toxicity endpoints.

2. Materials and methods

2.1. Material characterization

Three MLGs with different properties were purchased from Sigma Aldrich and labelled as G1, G2 and G3. The morphologies of three MLGs were characterized by transmission electron microscopy (TEM) imaging (Fig. 1). Atomic Force Microscopy (AFM) images were obtained using a multimode nanoscope V scanning probe microscopy system (NanoManVS, USA), followed by analyzing 80 discrete particles of MLGs using a NanoScope analysis software. The detailed information regarding TEM and AFM imaging is described in SI.

The average lateral sizes of G1, G2 and G3 were 7.4 ± 0.3, 6.4 ± 0.1 and 2.8 ± 0.1 μm, and the associated thicknesses were 5.0 ± 0.1, 4.2 ± 0.1 and 4.0 ± 0.2 nm, respectively, indicating reduced lateral size and layer number from G1 to G3 (Fig. 2). The dimension of a given MLG from AFM imaging was larger than that from TEM analysis; this is likely due to different aggregates targeted and we note that the relative size and thickness among three materials were consistent. The C, H and N content (by mass) of the MLGs were measured using a Vario EL CHN Elemental Analyzer (Germany). Their ash contents were determined by heating in a muffle furnace for 4 h at 900 °C. The oxygen content of these materials was calculated by mass balance. The (O + N)/C ratio for each MLG as a reflection of hydrophobicity was calculated, which followed a pattern of G1 > G2 > G3. The static contact angle of MLGs with water was determined with a contact angle analyzing system (KRUSS DSA100) to characterize their external hydrophobicity.

The surface area (SA) of these materials was obtained from the N_2 sorption-desorption isotherms at 77 K using an Autosorb-1-MP Surface Area Analyzer (Quantachrome Instruments, USA) after outgassing at 105 °C for 16 h. SA was estimated from N_2 sorption-desorption isotherms using the multipoint BET method. Selected physicochemical properties including elemental content, contact angle, and SA of G1, G2 and G3 are summarized in Table 1.

2.2. Soil and test organism

Two soils (referred to as potting soil and farm soil) were used to compare the possible difference in stress of MLG exposure to earthworms dwelling in soils with distinct properties. The farm soil was collected from a ranch near Houston, Texas, USA, and the potting soil (commonly used as soil amendment for organic gardening) was purchased from a local hardware store. Select agronomic soil properties were measured by the Soil Characterization Laboratory at Texas A&M University (Table S1). Both soils were air dried at room temperature (around 25 °C) for a week and passed through a 2.0 mm sieve before use.

Red worms (*Eisenia fetida*) were purchased from The Worm Farm in Durham, CA. Worms were maintained in a plastic box (60 L) with Sphagnum peat moss moistened to achieve a water content of approximately 35%. The box was loosely covered with a black plastic film to reduce water evaporation, and the thickness of peat moss was approximately 10 cm. The earthworms were fed every other day with Magic Worm Food (Magic Products Inc., Amherst Junction, WI), which contains 12% crude protein, 1% crude fat and 6% crude fiber. Specifically, the top 2 cm of peat moss was pushed aside to add 2-mm thick worm food (powder form) evenly, after that the peat moss was put back to cover the food and sprayed water. Sexually mature earthworms with a mass of 300−500 mg were selected for the MLG exposure test.

2.3. Avoidance test

Air-dried and sieved potting and farm soils were amended with individual MLGs (dry powders) at a concentration of 0.2% and 1% dry soil. The soil and MLG were thoroughly mixed with a spatula for 30 min, and then the bucket was sealed tightly and rolled back and forth for 30 min. The lower MLG concentration administered in this study is comparable to those in the existing relevant studies (Du et al., 2015; Holden et al., 2014). Relatively high MLG concentrations were also used to elicit a response and advance a mechanistic understanding of the mode of action. Such concentrations are unlikely to be found in soils impacted by incidental releases and would likely be found only at accidental release or disposal sites. The moisture content of each soil was adjusted to 60% of the corresponding water holding capacity (Kinney et al., 2012, detailed in SI).

Avoidance tests were conducted using a stainless-steel wheel as described by Li and Alvarez (2011). Control soil (100 g) without any amendment was added to three compartments of the avoidance wheel (Fig. 3), and the MLG-amended soil was transferred to the remaining three compartments. Ten earthworms with intact clitellum were added to the center of each avoidance wheel, and a lid was placed on the top to prevent worm escape. We observed that all earthworms disappeared from the center chamber within 1 min, indicating quick entry into the compartments. Three replicates were conducted for each treatment. The wheels were placed in the dark at 22 °C for 48 h. After the test, the lid was removed and aluminum plates were immediately inserted into the partitions between the compartments, thereby blocking the earthworms from moving after the test was completed. The number of earthworms in each compartment was recorded and the percentage of worms in MLG-free soil was calculated for each treatment.

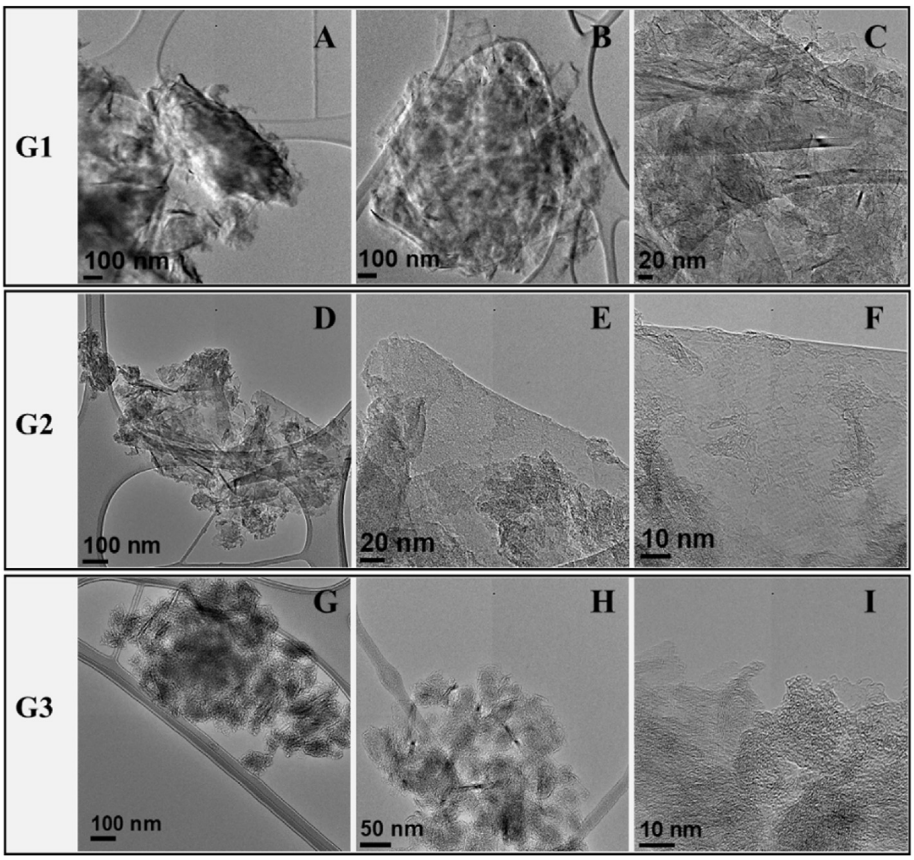

Fig. 1. Morphology of G1 (A, B, C), G2 (D, E, F) and G3 (G, H, I) observed by transmission electron microscopy (TEM).

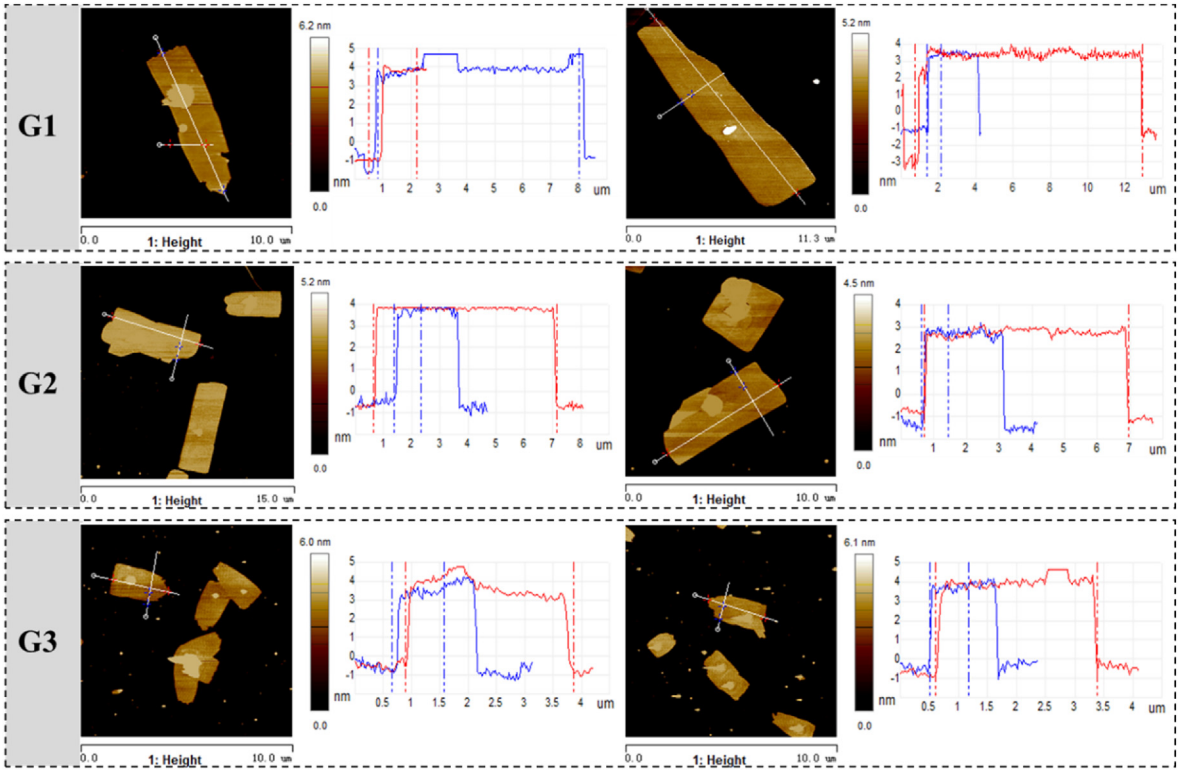

Fig. 2. Atomic Force Microscopy (AFM) images of G1, G2 and G3.

Table 1
Selected physicochemical properties of MLGs used in this work.

Material	Elemental composition (%)				Ash (%)	(O + N)/C	Contact angle (°)	Surface area (m^2/g)
	C	H	N	O				
G1	96.18	0.32	0.21	2.60	0.70	0.029	122.8	294.5
G2	94.91	0.29	0.27	3.91	0.63	0.044	118.8	467.0
G3	91.98	0.40	0.64	6.22	0.77	0.075	115.1	726.9

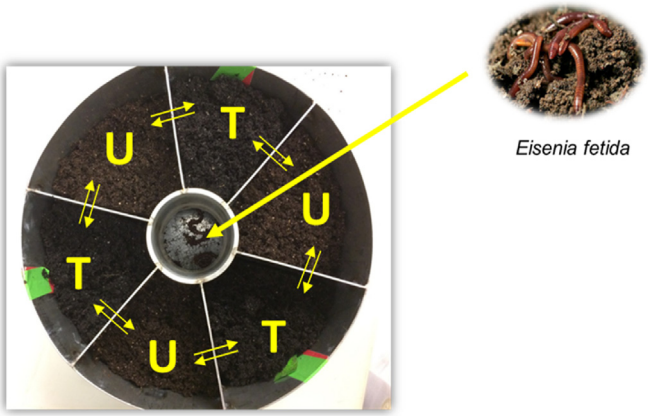

Fig. 3. Avoidance test wheel. "U" and "T" denote the un-amended soil and the treatments with MLGs, respectively. Earthworms were put at the center as the one-way arrow indicates. Two-way arrows between U and T indicate that earthworms can move freely between these compartments.

Earthworms that were cut into two pieces by the inserted plates were counted as 0.5 for each adjacent compartment.

2.4. Reproduction and oxidative stress

Earthworm exposure to MLGs (same concentrations as described in **2.3**) in both potting and farm soils were conducted in triplicate jars at 22 °C for 28 d. At the end of exposure, cocoons in each jar were counted, and the earthworms were transferred to a wet filter paper in the dark for 48 h for depuration. Two earthworms from each replicate were rinsed with Milli-Q water and weighed into a 5-mL centrifuge tube. The tube was amended with extraction medium (1:9, w/v) consisting of iced 50 mM Tris-HCl buffer, 250 mM sucrose and 1 mM EDTA (pH = 7.5). The worm tissues were thoroughly and quickly mixed in a mortar. The homogenate was centrifuged at 8000 rpm for 10 min at 4 °C, and the supernatant was sampled for biochemical assays. Specifically, tissue levels of superoxide dismutase (SOD), catalase (CAT), peroxidase (POD) activities, as well as malonaldehyde (MDA) and protein content, were determined using assay kits from Biovision (Milpitas, CA) and BioAssay Systems (Hayward, CA). All absorbance measurements were made on a multimode plate reader (Infinite M Plex, Tecan). The selected wavelengths for SOD, CAT, POD, MDA and protein tests were 440, 570, 570, 535 and 595 nm, respectively. Enzyme activities and MDA content were normalized by total protein content.

2.5. Survival rate and mitochondrial membrane potential of coelomocytes

The survival rate and mitochondrial membrane potential of coelomocytes were chosen as toxicity endpoints because (1) coelomocytes in earthworm coelom act as the immune defenders against environmental stress and are important in nutrition transport and xenobiotic metabolism (Gupta et al., 2014), and (2) mitochondria play a key role in cell energy conversion and storage, apoptosis and/or necrosis. Non-destructive extraction of earthworm coelomocytes was conducted as previously described (Eyambe, 1991). After 48 h depuration on a wet filter paper, two earthworms from each replicate were rinsed with Milli-Q water. Each worm was immediately added to 1.5 mL EP tube containing 1 mL extrusion medium (5% ethanol, 95% normal saline, 2.5 mg/mL EDTA and 10 mg/mL guaiacol glyceryl ether, pH = 7.38) for 3 min. Afterwards, earthworms were removed and the extrusion medium was centrifuged at 3000 rpm for 10 min (4 °C). The supernatant was discarded and the coelomocytes were rinsed twice with PBS buffer (4 °C). The cell number within each treatment was calculated by Hemocytometer and was adjusted to 4×10^5–5×10^5/mL for the following analysis.

The survival rate of coelomocytes was measured using a MTT cell proliferation assay kit (Biovision Inc., Milpitas, CA). Viable cells with active metabolism can convert the water soluble MTT (3-(4,5-dimethylthiazol-20yl)-2,5-diphenyltetrazolium bromide) to an insoluble formazan product. Mitochondrial membrane potential of the coelomocytes was evaluated using BioVision's TMRE (tetramethylrhodamine, ethyl ester) kit because TMRE is a red-orange cell-permeable dye that can be readily accumulated in active mitochondria.

2.6. Statistical analysis

Differences among the endpoints at the whole-organism, histological and cellular levels were analyzed using a two-way ANOVA with LSD (Least Significant Difference) and S–N–K (Student-Newman-Keuls) tests with SPSS 20.0 software (IBM Analytics), and were considered significant at $p < 0.05$.

3. Results and discussion

3.1. Earthworms avoided smaller and more hydrophilic MLGs and experienced a decrease in cocoon formation

Earthworms have highly discriminatory sensory neurons that respond to tactile and chemical stimuli, thus navigating and manipulating their environment (Novo et al., 2015; Shoults-Wilson et al., 2011). Dopaminergic sensory cells distributed in the epidermis of earthworms transfer sensory information to the ventral nerve cord and activate the dorsal giant fibers and motor neurons that control rapid reflexes (Gong et al., 2012). In this study, earthworms significantly avoided the potting soil with 1% MLGs (Fig. 4A); G1, G2, and G3 amendment increased the worm numbers in the unexposed soil control by 40.0, 77.1 and 78.5%, respectively. As for the farm soil, worms significantly avoided 1% of G2 and G3 (but not G1), with worm numbers increased by 51.5 and 33.3% relative to the control, respectively.

Earthworms avoided G2 and G3 to a greater extent than G1. It is known that earthworms can distinguish between food based on size, shape and texture (Shoults-Wilson et al., 2011). In this study, G2 and G3 are more hydrophilic as indicated by their higher

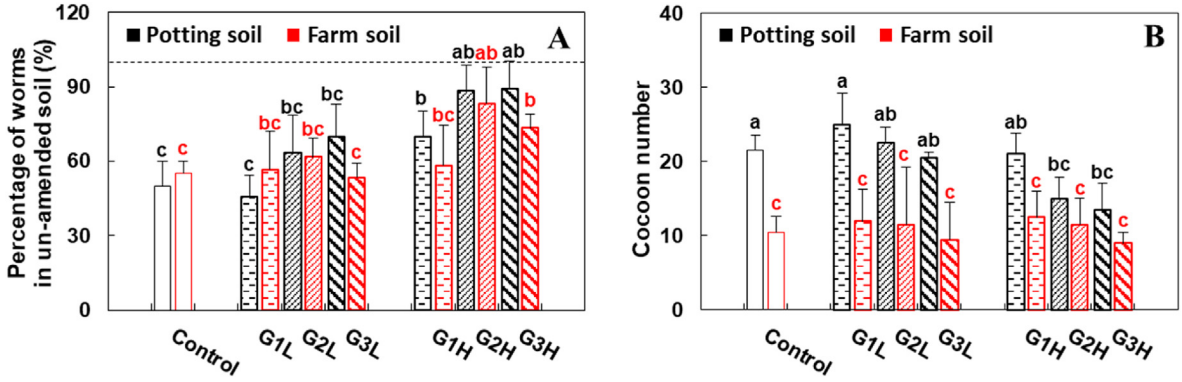

Fig. 4. Percentages of earthworms in un-amended potting and farm soils after 48 h avoidance test (A, the dotted line denotes 100%). Earthworms avoided G2 and G3 amended in both soils at 1%. Cocoon numbers, which were greater in potting soil in the presence of G1 than G2 or G3 on 28 d (B). "Control" denotes that the T treatment in Fig. 3 is the soil without any amendment. G1L, G2L and G3L denote T treatments of soil amended with 0.2% of MLG; G1H, G2H and G3H denote those amended with 1% of MLG. Column values marked with the same letter are not statistically significant ($p < 0.05$).

(O + N)/C ratios (0.044, 0.075 and 0.029, respectively) and lower contact angles (118.8, 115.1, and 122.8°, respectively) than G1, making them more bioavailable to earthworms. The smaller size and dissimilar aggregate shapes of G2 and G3 (Figs. 1 and 2) may also contribute to the differences in avoidance behavior, although a clear etiology remains to be established. A study on microplastic transport by earthworms (*Lumbricus terrestris* L.) revealed that only two smaller polystyrene microbeads (710–850 μm and 1180–1400 μm) were detected in worm casts, while no larger ones were observed (Rillig et al., 2017). This indicated that earthworms can discriminate foods with different sizes, and the carbonaceous materials with smaller size seem to be more bioavailable to earthworms.

Please note that heteroaggregation of graphene with soil particles or naturally occurring dissolved organic colloids and minerals has been reported (Huang et al., 2016; Sotirelis and Chrysikopoulos, 2017; Wang et al., 2015). This common phenomenon could influence the bioavailability and impact of graphene to earthworms (Li et al., 2010), which underscores the need for advancing analytic techniques for characterizing heteroaggregation in complex matrices (including soils) to better understand the fate and ecotoxicity of such materials.

All earthworms survived the 28-d exposure without supplemental feeding. With the increasing avoidance by the smaller and more hydrophilic MLGs, cocoon numbers in the potting soil were higher in the presence of G1 than G2 or G3 at both exposure levels (Fig. 4B). This trend was more pronounced at high MLG concentrations, with cocoon numbers decreased by 30.2 and 37.2% in G2 and G3 at 1%, respectively. Cocoon counts in the farm soil tended to be inhibited by G2 and G3, although the effect was not statistically significant. A small decline in earthworm cocoons could significantly impact the population size and structure (Jager et al., 2006).

3.2. Larger and more hydrophobic MLGs exerted a higher oxidative stress

When considering the morphology and hydrophobicity character, the antioxidative responses of worms to MLG exposure was dissimilar to those impacts on the whole organism, including avoidance and reproduction. MLGs (G1 and G2) with a larger size and greater hydrophobicity induced oxidative stress and peroxide generation in earthworms. Specifically, in the potting soil, G2 at 1% significantly increased SOD activity by 57.3% (Fig. 5A), leading to hydrogen peroxide generation. CAT activity was enhanced to capture peroxides upon exposure to 1% G2, although the effect was not statistically significant (Fig. 5B). POD activity was not impacted under all MLG treatments (Fig. 5C). However, as a result of the overall defensive activities, G2 at 1% significantly increased the worm MDA content by 52.7% (Fig. 5D), indicating that significant stress resulted in cell membrane damage in earthworms. In the farm soil, G2 at 0.2%, as well as G1 and G2 at 1%, significantly enhanced SOD activity by 47.1, 49.9 and 52.6%, respectively (Fig. 5A). CAT activity was insignificantly increased upon exposure to G2 at both levels (Fig. 5B); however, POD activities upon exposure to 0.2% G2, as well as 1% G1 and G2 were 2.0–2.8 fold higher than that in the control (Fig. 5C). Nevertheless, these enzymes failed to completely alleviate the oxidative stress, leading to 63.8–98.7% increase in worm MDA content exposed to both G1 and G2 at two levels (Fig. 5D).

Overall, G3 had a little effect on the earthworms' antioxidative systems, while G1 and G2 posed significant oxidative stress. Such a difference was largely attributable to the larger size and greater hydrophobicity of G1 and G2. Specifically, G1 is likely to form bulk structure with multiple sheets (5.0 ± 0.1 nm) stacked together; its average lateral size approached 7.4 ± 0.3 μm (Figs. 1 and 2). G2 had thinner sheets of 4.2 ± 0.1 nm, and the lateral size (6.4 ± 0.1 μm) was only slightly lower than that of G1 (Figs. 1 and 2). Moreover, G1 and G2 were more hydrophobic than G3 (with (O + N)/C ratios being 0.029, 0.044, and 0.075, respectively; contact angles being 122.8, 118.8, and 115.1°, respectively), making them less readily absorbed by worm tissues. A larger dimension and higher hydrophobicity could facilitate adherence to the worm tissue surface, leading to oxidative stress and subsequent dysfunction of cell membranes. Lammel et al. (2013) found that larger micro-sized graphene platelets were retained by the microvilli of the cell membrane. Wang et al. (2013) found that the sheet structure of graphene acted as an efficient support for anammox bacteria to form biofilms, which means the specific lateral dimension of graphene has a close affinity with cell membranes.

Interestingly, SOD and POD activities of earthworms in two soils were negatively correlated with worm cocoon numbers ($p < 0.01$), suggesting an activation of the defense system and a suppression of worm reproduction upon MLG exposure. Therefore, these two histological parameters can be used as an indicator for the assessment of worm reproductive activity in the case with MLG exposure. Oxidative stress in the farm soil was more pronounced than that in the potting soil, which is probably due to much lower organic carbon content in farm soil (0.025 vs. 0.4 in potting soil) leading to higher MLG bioavailability (Table S1).

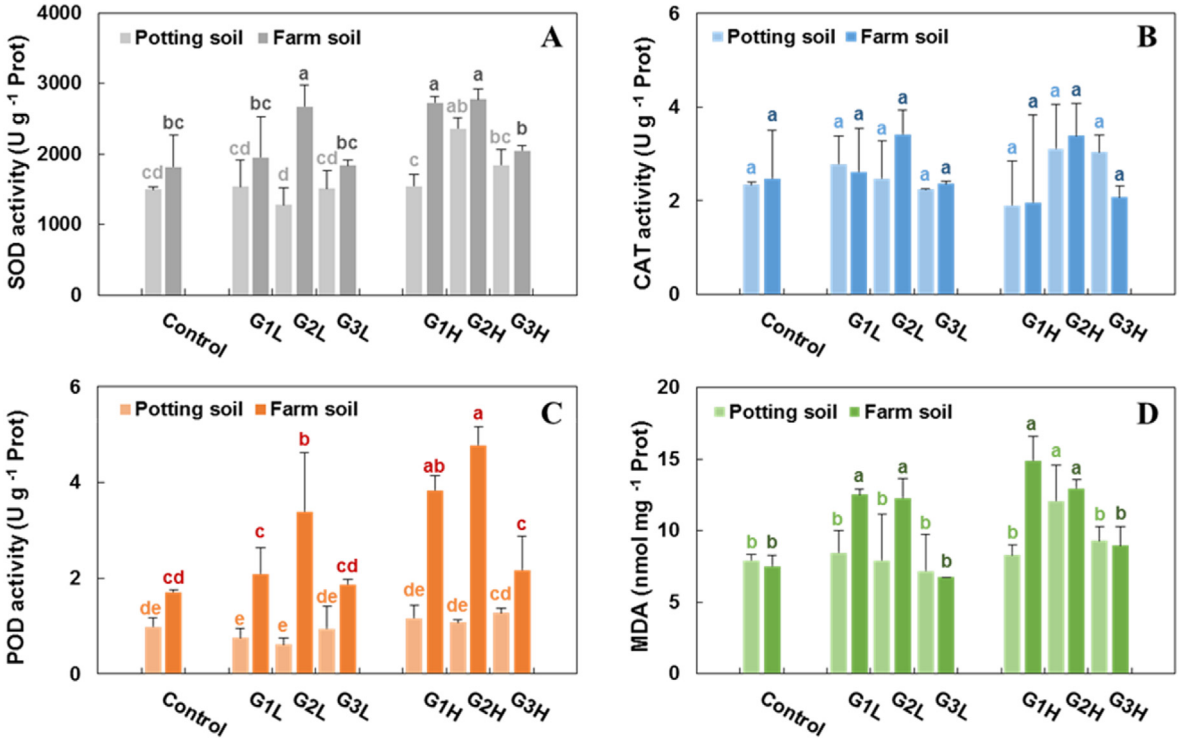

Fig. 5. SOD (superoxide dismutase, A), CAT (catalase, B) and POD (peroxidase, C) activities, as well as MDA content (malonaldehyde, D) in earthworms exposed to G1, G2 or G3 for 28 d. Earthworms exposed to G1 or G2 experienced oxidative stress and peroxide generation in both soils. "Control" denotes the soil without any amendment. G1L, G2L and G3L denote soil amended with 0.2% of MLG; G1H, G2H and G3H denote soil amended with 1% of MLG. Column values marked with the same letter are not statistically significant ($p < 0.05$).

3.3. Smaller and more hydrophilic MLGs had a negative effect on survival and mitochondrial activity of coelomocytes

In both potting and farm soils, G3 at both concentrations reduced the survival rate of coelomocytes by 20.2–56.0% (Fig. 6A). Although the effects of G1 and G2 on coelomocyte survival were different between two soils, G3 suppressed survival in both soils. Cellular and subcellular effects of MLGs are significantly influenced by their absorption potential. G3 was present as fragments and had the smallest lateral size (2.8 ± 0.1 μm) and thickness (4.0 ± 0.2 nm) among the three MLGs tested (Figs. 1 and 2). In addition, G3 possessed the highest (O + N)/C ratio (0.075) and lowest contact angle (115.1°) and thus (Table 1), was most bioavailable to earthworms. This dimensional and hydrophilic character likely facilitated entry into the worm coelom through dorsal pores that connect to the exterior. Zhou et al. (2019) revealed that the dorsal pore is an important absorption pathway for petroleum hydrocarbon uptake by *Eisenia fetida*. When experiencing stress from a mechanical or chemical stimuli, worms can enlarge the pores, which in turn may increase possibility of the uptake of MLGs with a relatively small size. Once MLG enters the dorsal pores, the particles may interact with numerous coelomocytes in coelomic fluids and directly impact cell viability. MLG can also enter the coelom through digestive absorption and the subsequent release to the circulatory system (Gupta et al., 2014). G3 was the most hydrophilic material tested, and its lateral size and thickness were smaller than

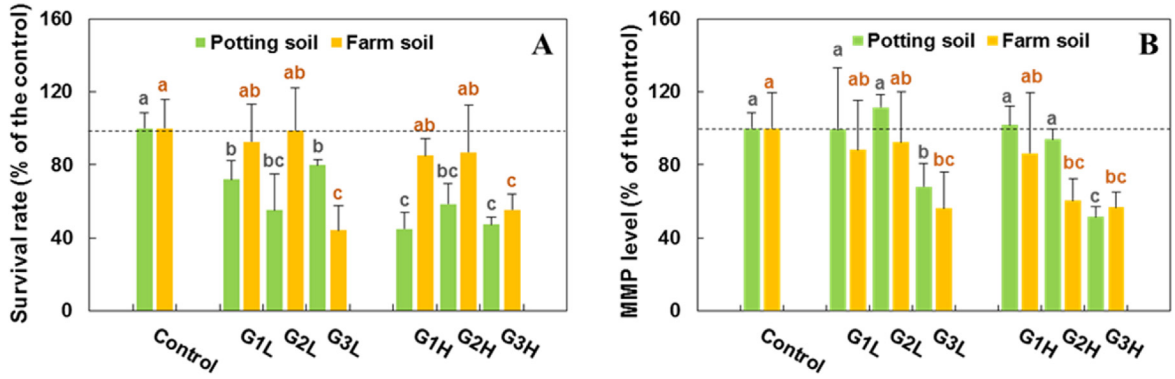

Fig. 6. Survival rate (A) and MMP level (mitochondrial membrane potential, B) of coelomocytes in earthworms exposed to G1, G2 and G3 for 28 d (dotted line denoting 100%). G3 inhibited both survival and MMP of coelomocytes in earthworms. "Control" denotes the soil without any amendment. G1L, G2L and G3L denote soil amended with 0.2% of MLG; G1H, G2H and G3H denote soil amended with 1% of MLG. Column values marked with the same letter are not statistically significant ($p < 0.05$).

the intestinal cells observed in *Eisenia fetida* by Wu et al. (2012). These characters led to the greatest absorption potential thereby exhibiting the highest cell toxicity.

More importantly, G3 posed a greater risk in hindering energy production, metabolism and signal transduction in worm cells. Specifically, G3 most significantly decreased the mitochondrial membrane potential (MMP) of the coelomocytes by 32.0–48.5% in both soils, leading to the largest disruption of the electron transport chain within worm immune cells (Fig. 6B). G3 is much larger than the mitochondria observed in *Eisenia fetida* (Wu et al., 2012), which likely yields a high probability of interaction with this important organelle. It has previously been documented that mitochondrial membrane potential in human cells was reduced by nano-sized graphene, nanographene oxides and graphene quantum dots and that the reduction was a function of exposure dose and duration (Chatterjee et al., 2014; Lammel et al., 2013; Qin et al., 2015). Interestingly, the mitochondrial membrane potential in worm coelomocytes from all treatments was positively correlated with that of cocoon numbers ($p < 0.05$), suggesting a close relationship between the energy production in worm coelomocytes and its reproductive potential.

4. Conclusions

Soils with high GBN concentrations (e.g., 1%) may disrupt earthworm populations and experience ecological imbalance. Importantly, disruption of the coelomocytes function following exposure to small and hydrophilic MLGs indicates a potential risk to the capability of earthworms to defend against xenobiotics. Antioxidative enzymes and lipid peroxides induced by large and hydrophobic MLGs indicated a damaged (permeabilized) membrane with compromised ability to serve as a barrier for contaminant penetration. Correlation between histological SOD/POD activity, as well as MMP of coelomocytes, and cocoon formation, underlined a close relationship between antioxidative activities or energy production with reproductive efficacy. Multiple biological responses ranging from the whole-organism to subcellular level revealed dissimilar effects of GBNs on earthworms as a function of MLG properties (e.g., morphology and hydrophobicity). This highlights the importance of these properties in determining absorption potential of GBNs and their interaction with earthworm membranes, and also suggests a need to consider multiple endpoints in assessing the ecological risks of these materials.

Author statement

All authors contributed to the manuscript.

Declaration of competing interest

The authors declare no conflicts of interest.

Acknowledgments

We thank Jacques Mathieu for providing the farm soil. We also thank Pingfeng Yu and Danning Zhang for their technical support of TEM observation, and Wen Song for her assistance with the avoidance experiment. We appreciate Dr. Jason C. White for constructive comments on this manuscript. This research was supported by the National Science Fund for Distinguished Young Scientist of China (41525005), National Natural Science Foundation of China (41821005 and 41629101), and the 111 Program (B14001).

Appendix A. Supplementary data

Supplementary data to this article can be found online at https://doi.org/10.1016/j.envpol.2020.114468.

References

Akhavan, O., Ghaderi, E., Akhavan, A., 2012. Size-dependent genotoxicity of graphene nanoplatelets in human stem cells. Biomaterials 33, 8017–8025.
Al-Hartomy, O.A., Khasim, S., Roy, A., Pasha, A., 2018. Highly conductive polyaniline/graphene nano-platelet composite sensor towards detection of toluene and benzene gases. Appl. Phys. A 125 article number: 12.
Calisi, A., Grimaldi, A., Leomanni, A., Lionetto, M.G., Dondero, F., Schettino, T., 2016. Multibiomarker response in the earthworm *Eisenia fetida* as tool for assessing multi-walled carbon nanotube ecotoxicity. Ecotoxicology 25, 677–687.
Chatterjee, N., Eom, H.J., Choi, J., 2014. A systems toxicology approach to the surface functionality control of graphene-cell interactions. Biomaterials 35, 1109–1127.
Du, J., Hu, X., Zhou, Q., 2015. Graphene oxide regulates the bacterial community and exhibits property changes in soil. RSC Adv. 5, 27009–27017.
Eyambe, 1991. A non-invasive technique for sequential collection of earthworm (*Lumbricus terrestris*) leukocytes during subchronic immunotoxicity studies. Lab. Anim. 25, 61–67.
Gomes, R.N., Borges, I., Pereira, A.T., Maia, A.F., Pestana, M., Magalhães, F.D., Pinto, A.M., Gonçalves, I.C., 2018. Antimicrobial graphene nanoplatelets coatings for silicone catheters. Carbon 139, 635–647.
Gong, P., Guan, X., Pirooznia, M., Liang, C., Perkins, E.J., 2012. Gene expression analysis of CL-20-induced reversible neurotoxicity reveals GABAA receptors as potential targets in the earthworm *Eisenia fetida*. Environ. Sci. Technol. 46, 1223–1232.
Gupta, S., Kushwah, T., Yadav, S., 2014. Earthworm coelomocytes as nanoscavenger of ZnO NPs. Nanoscale Res. Lett. 9 article number: 259.
Holden, P.A., Klaessig, F., Turco, R.F., Priester, J.H., Rico, C.M., Avila-Arias, H., Mortimer, M., Pacpaco, K., Gardea-Torresdey, J.L., 2014. Evaluation of exposure concentrations used in assessing manufactured nanomaterial environmental hazards: are they relevant? Environ. Sci. Technol. 48, 10541–10551.
Huang, G.X., Guo, H.Y., Zhao, J., Liu, Y.H., Xing, B.S., 2016. Effect of co-existing kaolinite and goethite on the aggregation of graphene oxide in the aquatic environment. Water Res. 102, 313–320.
Huang, X., Chen, X., Li, A., Atinafu, D., Gao, H., Dong, W., Wang, G., 2019. Shape-stabilized phase change materials based on porous supports for thermal energy storage applications. Chem. Eng. J. 356, 641–661.
Jager, T., Reinecke, S.A., Reinecke, A.J., 2006. Using process-based modelling to analyse earthworm life cycles. Soil Biol. Biochem. 38, 1–6.
Katsumiti, A., Tomovska, R., Cajaraville, M.P., 2017. Intracellular localization and toxicity of graphene oxide and reduced graphene oxide nanoplatelets to mussel hemocytes in vitro. Aquat. Toxicol. 188, 138–147.
Kinney, T.J., Masiello, C.A., Dugan, B., Hockaday, W.C., Dean, M.R., Zygourakis, K., Barnes, R.T., 2012. Hydrologic properties of biochars produced at different temperatures. Biomass Bioenergy 41, 34–43.
Lammel, T., Boisseaux, P., Fernández-Cruz, M.L., Navas, J.M., 2013. Internalization and cytotoxicity of graphene oxide and carboxyl graphene nanoplatelets in the human hepatocellular carcinoma cell line Hep G2. *Part*. Fibre Toxicol. 10 article number: 27.
Li, D., Alvarez, P.J.J., 2011. Avoidance, weight loss, and cocoon production assessment for *Eisenia fetida* exposed to C_{60} in soil. Environ. Toxicol. Chem. 30, 2542–2545.
Li, D., Fortner, J.D., Johnson, D.R., Chen, C., Li, Q., Alvarez, P.J.J., 2010. Bioaccumulation of $^{14}C_{60}$ by the earthworm *Eisenia fetida*. Environ. Sci. Technol. 44, 9170–9175.
Lu, K., Dong, S., Petersen, E.J., Niu, J., Chang, X., Wang, P., Lin, S., Gao, S., Mao, L., 2017. Biological uptake, distribution, and depuration of radio-labeled graphene in adult zebrafish: effects of graphene size and natural organic matter. ACS Nano 11, 2872–2885.
Malina, T., Maršálková, E., Holá, K., Tuček, J., Scheibe, M., Zbořil, R., Maršálek, B., 2019. Toxicity of graphene oxide against algae and cyanobacteria: nanoblade-morphology-induced mechanical injury and self-protection mechanism. Carbon 155, 386–396.
Mao, L., Liu, C., Lu, K., Su, Y., Gu, C., Huang, Q., Petersen, E.J., 2016. Exposure of few layer graphene to *Limnodrilus hoffmeisteri* modifies the graphene and changes its bioaccumulation by other organisms. Carbon 109, 566–574.
Novo, M., Lahive, E., Díez-Ortiz, M., Matzke, M., Morgan, A.J., Spurgeon, D.J., Svendsen, C., Kille, P., 2015. Different routes, same pathways: molecular mechanisms under silver ion and nanoparticle exposures in the soil sentinel *Eisenia fetida*. Environ. Pollut. 205, 385–393.
Pakarinen, K., Petersen, E.J., Leppänen, M.T., Akkanen, J., Kukkonen, J.V.K., 2011. Adverse effects of fullerenes (nC_{60}) spiked to sediments on *Lumbriculus variegatus* (Oligochaeta). Environ. Pollut. 159, 3750–3756.
Peruzynska, M., Cendrowski, K., Barylak, M., Tkacz, M., Piotrowska, K., Kurzawski, M., Mijowska, E., Drozdzik, M., 2017. Comparative in vitro study of single and four layer graphene oxide nanoflakes- Cytotoxicity and cellular uptake. Toxicol. Vitro 41, 205–213.
Qin, Y., Zhou, Z.W., Pan, S.T., He, Z.X., Zhang, X., Qiu, J.X., Duan, W., Yang, T., Zhou, S.F., 2015. Graphene quantum dots induce apoptosis, autophagy, and inflammatory response via p38 mitogen-activated protein kinase and nuclear factor-κB mediated signaling pathways in activated THP-1 macrophages.

Toxicology 327, 62–76.
Rillig, M.C., Ziersch, L., Hempel, S., 2017. Microplastic transport in soil by earthworms. Sci. Rep. 7 article number: 1362.
Scott-Fordsmand, J.J., Krogh, P.H., Schaefer, M., Johansen, A., 2008. The toxicity testing of double-walled nanotubes-contaminated food to *Eisenia veneta* earthworms. Ecotoxicol. Environ. Saf. 71, 616–619.
Shoults-Wilson, W.A., Zhurbich, O.I., McNear, D.H., Tsyusko, O.V., Bertsch, P.M., Unrine, J.M., 2011. Evidence for avoidance of Ag nanoparticles by earthworms (*Eisenia fetida*). Ecotoxicology 20, 385–396.
Sotirelis, N.P., Chrysikopoulos, C.V., 2017. Heteroaggregation of graphene oxide nanoparticles and kaolinite colloids. Sci. Total Environ. 579, 736–744.
Wang, D., Wang, G., Zhang, G., Xu, X., Yang, F., 2013. Using graphene oxide to enhance the activity of anammox bacteria for nitrogen removal. Bioresour. Technol. 131, 527–530.
Wang, H.T., Adeleye, A.S., Huang, Y.X., Li, F.T., Keller, A.A., 2015. Heteroaggregation of nanoparticles with biocolloids and geocolloids. Adv. Colloid Interface Sci. 226, 24–36.
Wu, S.J., Zhang, H., Hu, Y., Li, H.L., Chen, J.M., 2012. Effects of 1,2,4-trichlorobenzene on the enzyme activities and ultrastructure of earthworm *Eisenia fetida*. Ecotoxicol. Environ. Saf. 76, 175–181.
Yang, G., Chen, C., Yu, Y., Zhao, H., Wang, W., Wang, Y., Cai, L., He, Y., Wang, X., 2018. Combined effects of four pesticides and heavy metal chromium (VI) on the earthworm using avoidance behavior as an endpoint. Ecotoxicol. Environ. Saf. 157, 191–200.
Zhou, W., Liang, J., Pan, H., Liu, J., Liu, Y., Zhao, Y., 2019. A model of the physiological and biochemical characteristics of earthworms (*Eisenia fetida*) in petroleum-contaminated soil. Ecotoxicol. Environ. Saf. 174, 459–466.
Zhu, C., Liu, F., Ling, C., Jiang, H., Wu, H., Li, A., 2019. Growth of graphene-supported hollow cobalt sulfide nanocrystals via MOF-templated ligand exchange as surface-bound radical sinks for highly efficient bisphenol A degradation. Appl. Catal. B Environ. 242, 238–248.